Audio-Magnetotelluric (AMT) Soundings across the Margin of the Chesapeake Bay Impact Structure, York-James and Middle Peninsulas, Virginia

By Herbert A. Pierce

Chapter J of
**Studies of the Chesapeake Bay Impact Structure—
The USGS-NASA Langley Corehole, Hampton, Virginia, and
Related Coreholes and Geophysical Surveys**

Edited by J. Wright Horton, Jr., David S. Powars, and Gregory S. Gohn

Prepared in cooperation with the
Hampton Roads Planning District Commission,
Virginia Department of Environmental Quality, and
National Aeronautics and Space Administration Langley Research Center

Professional Paper 1688

U.S. Department of the Interior
U.S. Geological Survey

Contents

Figures

Table

Audio-Magnetotelluric (AMT) Soundings across the Margin of the Chesapeake Bay Impact Structure, York-James and Middle Peninsulas, Virginia

By Herbert A. Pierce[1]

Abstract

The Chesapeake Bay impact structure is a roughly circular subsurface feature created about 35 million years ago when a comet fragment or asteroid impacted the continental shelf near the present-day mouth of the Chesapeake Bay. Interpretation of seismic and other data suggests that the central crater is about 35 to 40 kilometers (km; 22 to 25 miles (mi)) wide and contains a central uplift. The central crater is surrounded by an annular trough that is about 25 km (16 mi) wide. The annular trough is surrounded by an outer fracture zone that is about 35 km (22 mi) wide.

During 2000 and 2001, 18 audio-magnetotelluric (AMT) soundings were collected across the western outer margin of the annular trough in two locations as part of the Chesapeake Bay impact crater study. These tensor AMT soundings provided estimates of impedances across the outer margin of the impact structure. From the impedances, resistivities and phases as a function of frequency were calculated. They were inverted as a function of depth, and electrical cross sections were constructed to provide an image of the electrical response associated with the structure.

The cross sections show a nearly vertical resistivity high at the outer margin of the annular trough. The bottoms of the electrical sections show a subhorizontal resistive layer interpreted to be the basement rocks buried by conductive sedimentary rocks. Polar plots of the tensor impedances were calculated, and the principal impedance directions indicate fracture orientations roughly parallel to the outer margin. The maximum depth of investigation for the soundings and sections is about 1,000 meters (m; about 3,300 feet (ft)) except inside the outer margin near Mathews, Va., where low-resistivity sediments limit the depth of exploration in some places to 300 m (980 ft).

[1]U.S. Geological Survey, Reston, VA 20192.

Introduction

The Chesapeake Bay impact structure is a subsurface feature of the eastern Virginia Coastal Plain and inner continental shelf (Powars and Bruce, 1999; Powars, 2000). It was formed about 35 million years ago by a comet fragment or asteroid impact on the late Eocene continental shelf. The feature was buried beneath several hundred meters of upper Eocene through Quaternary marine and paralic sediments.

The structure has a central crater that underlies the southern Delmarva Peninsula. The margin of the central crater separates the central crater from the less deformed annular trough and is about 35 to 40 kilometers (km; 22 to 25 miles (mi)) in diameter. A small central uplift within the central crater is inferred from geophysical evidence (Poag, Hutchinson, and others, 1999; Poag, Plescia, and Molzer, 1999).

The annular trough extends from the margin of the central crater outward to the faulted outer margin, a radial distance of about 25 km (16 mi) (Poag, 1996). The outer margin has a diameter between 85 and 90 km (53 and 56 mi). The annular trough is surrounded by an outer fracture zone that is about 35 km (22 mi) wide (Powars, 2000; Horton and others, this volume, chap. A, fig. A1).

The Chesapeake Bay impact structure resulted from a wet-target impact; the target included water-saturated sediments and a seawater column (Horton and others, this volume, chap. A). Crater collapse was probably accompanied by the catastrophic resurge of water-sediment-ejecta mixtures toward the center of the crater, which resulted in local erosion of the outer crater margin and adjacent sediments and deposition within the crater (Gohn and others, this volume, chap. C). These sediments were reworked by wave swash and impact-generated tsunamis as the sea returned to equilibrium (Gohn and others, this volume, chap. C). The Exmore beds are interpreted to be the sedimentary deposits produced by the inward-flowing resurge of bottom currents following collapse of the water column and perhaps by the return of impact-produced tsunamis (Gohn and others, this volume, chap. C).

During 2000 and 2001, 18 audio-magnetotelluric soundings were collected across the western outer margin of the annular trough in two locations (figs. J1 and J2, table J1). The work was part of the Chesapeake Bay impact crater study conducted by the U.S. Geological Survey (USGS) and its partners (see "Acknowledgments"). The purpose of the electromagnetic soundings was to test the ability of the audio-magnetotelluric technique to image the electrical nature of the outer margin of the Chesapeake Bay impact structure. Specifically, this work was designed to help map the outer margin, measure the magnitude of electrical anisotropy, and provide impedance strike directions. Because most of the impact structure is covered by the lower Chesapeake Bay, these soundings were focused on the western outer margin, collapse structures in the annular trough, and the underlying crystalline basement rocks. The data from the soundings supplement data from seismic surveys and deep coreholes, including the USGS-NASA Langley corehole (fig. J2) discussed in other chapters of this volume.

Audio-Magnetotelluric Methods

Audio-magnetotelluric (AMT) soundings are made to determine variations in the electrical resistivity of the earth with depth (Cagniard, 1950, 1953; Wait, 1962; Keller and Frischknecht, 1966; Hoover and Long, 1976; Hoover and others, 1976, 1978; Dmitriev and Berdichevsky, 1979; Vozoff, 1986, 1991). The AMT method uses natural-source multifrequency electromagnetic signals that result from lightning or atmospheric disturbances ("sferics") as an energy source. For this survey, a controlled-source transmitter was used to supplement natural source energy when signal strength was low. Low levels of natural source energy in the middle frequency band of the instrument can cause errors in the impedance estimates.

AMT soundings consist of electrical and magnetic field measurements over a range of frequencies from 5 to 100,000 hertz (Hz) with fixed receiver and transmitter locations. The distribution of currents induced in the earth depends on the earth's electrical resistivity, the earth's magnetic permeability, and the frequency measured. Because low-frequency signals penetrate to greater depths than high-frequency signals, measurements of the electromagnetic response at several frequencies contain information on the variation of resistivity with depth. In this study, a series of soundings were stitched together to form two profiles or lines approximately normal to the outer margin structure.

Field Work

AMT tensor soundings collected during the spring of 2000 on the York-James Peninsula (fig. J2) were recorded by using an Electromagnetic Instruments, Inc. (EMI), 10-channel MT1 system. For each station location, approximately 55 AMT frequencies were recorded for each of the two directions (*Ex* and *Ey*) from 4 to 23,250 Hz.

The soundings collected during the spring of 2001 on the Middle Peninsula (fig. J2) were recorded by using a Geometrics EH4 system. Approximately 40 AMT frequencies were collected with this system for each of the two directions from 10 to 100,000 Hz. The magnetic field sensors, electrical field sensors, buffers, and preamplifiers for both systems were manufactured by EMI.

Tensor Audio-Magnetotelluric Soundings

The impedance tensor (Z) is frequency dependent and is obtained from vector measurements of the electrical and magnetic fields. The AMT method measures both orthogonal magnetic and electrical fields (*Hx, Hy, Ex,* and *Ey*) so that the impedance can be described as a complex tensor to account for anisotropy.

The AMT impedance tensor (Z) contains four complex components that relate the measured electrical (E) and magnetic (H) fields:

$$\begin{bmatrix} Ex \\ Ey \end{bmatrix} = \begin{bmatrix} Zxx & Zxy \\ Zyx & Zyy \end{bmatrix} \times \begin{bmatrix} Hx \\ Hy \end{bmatrix} \quad (1)$$

The impedances are computed from spectra collected in the field by using a magnetic (H) field reference where $<AB^*>$ is a complex value formed from the real and imaginary parts of AB. The quantity $<AA^*>$ is an autopower and is real valued. Both the scalar and tensor impedance values are frequency averaged from the spectral data.

$$Zxx = \frac{<ExHx^*><HyHy^*> - <ExHy^*><HyHx^*>}{<HxHx^*><HyHy^*> - <HxHy^*><HyHx^*>} \quad (2)$$

$$Zxy = \frac{<ExHx^*><HxHy^*> - <ExHy^*><HxHx^*>}{<HyHx^*><HxHy^*> - <HyHy^*><HxHx^*>} \quad (3)$$

$$Zyx = \frac{<EyHx^*><HyHy^*> - <EyHy^*><HyHx^*>}{<HxHx^*><HyHy^*> - <HxHy^*><HyHx^*>} \quad (4)$$

$$Zyy = \frac{<EyHx^*><HxHy^*> - <EyHy^*><HxHx^*>}{<HyHx^*><HxHy^*> - <HyHy^*><HxHx^*>} \quad (5)$$

All of the soundings collected use local *Hx* and *Hy* fields as reference (Gamble and others, 1979a,b).

The apparent resistivities and phases are computed from the four components of the impedance tensor (*Zxx, Zxy, Zyx,* and *Zyy*). Apparent resistivities $\rho(f)$ and corresponding phases $\phi(f)$ are computed by using:

$$\rho_{ij} = \frac{1}{5f}|Z_{ij}|^2 \quad (6)$$

$$\phi_{ij} = \tan^{-1}\left(\frac{im\{Z_{ij}\}}{re\{Z_{ij}\}}\right) \quad (7)$$

where *im* is the imaginary part and *re* is the real part of Z.

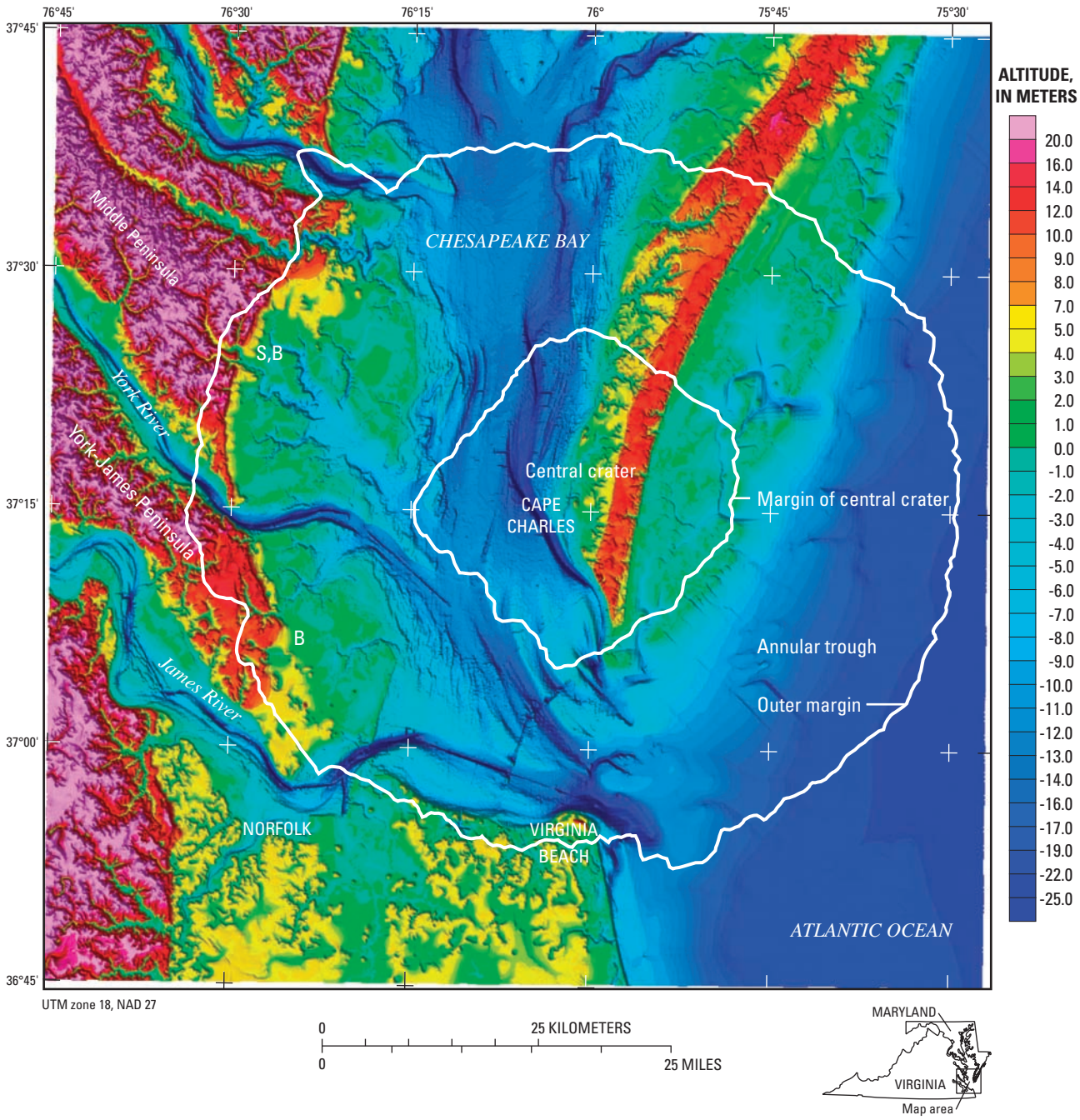

Figure J1. Color shaded-relief map of the part of Virginia near the mouth of Chesapeake Bay showing the location of the subsurface Chesapeake Bay impact structure. The land part of the map is from the U.S. Geological Survey's National Elevation Dataset digital elevation model (DEM). The bathymetry is from the National Oceanic and Atmospheric Administration (NOAA), National Geophysical Data Center (NGDC), U.S. coastal relief model. The original data resolution of the DEM grid was 30 m (98 ft), but data were regridded to 60 m (197 ft) and merged with the NOAA bathymetric data. The Suffolk-Big Bethel (S, B) scarp is visible in the center-left portion of the map; the resolution is not sufficient to identify the Harpersville scarp (Johnson and others, 2001). All three scarps are shown in Horton and others (this volume, chap. A, fig. A4). Locations of the central crater and outer margin of the Chesapeake Bay impact structure are from Powars and Bruce (1999). The AMT data indicate that the Suffolk-Big Bethel scarp is coincident with the westernmost edge of the outer margin of the impact structure across the Middle Peninsula. The Big Bethel scarp on the York-James Peninsula does not coincide with the location of the outer margin suggested by the AMT data, which is the same location suggested by Powars and Bruce (1999). The scarp is about 2.5 km (about 1.6 mi) northeast of the resistivity high interpreted to be the outer margin according to the AMT data and Powars and Bruce (1999).

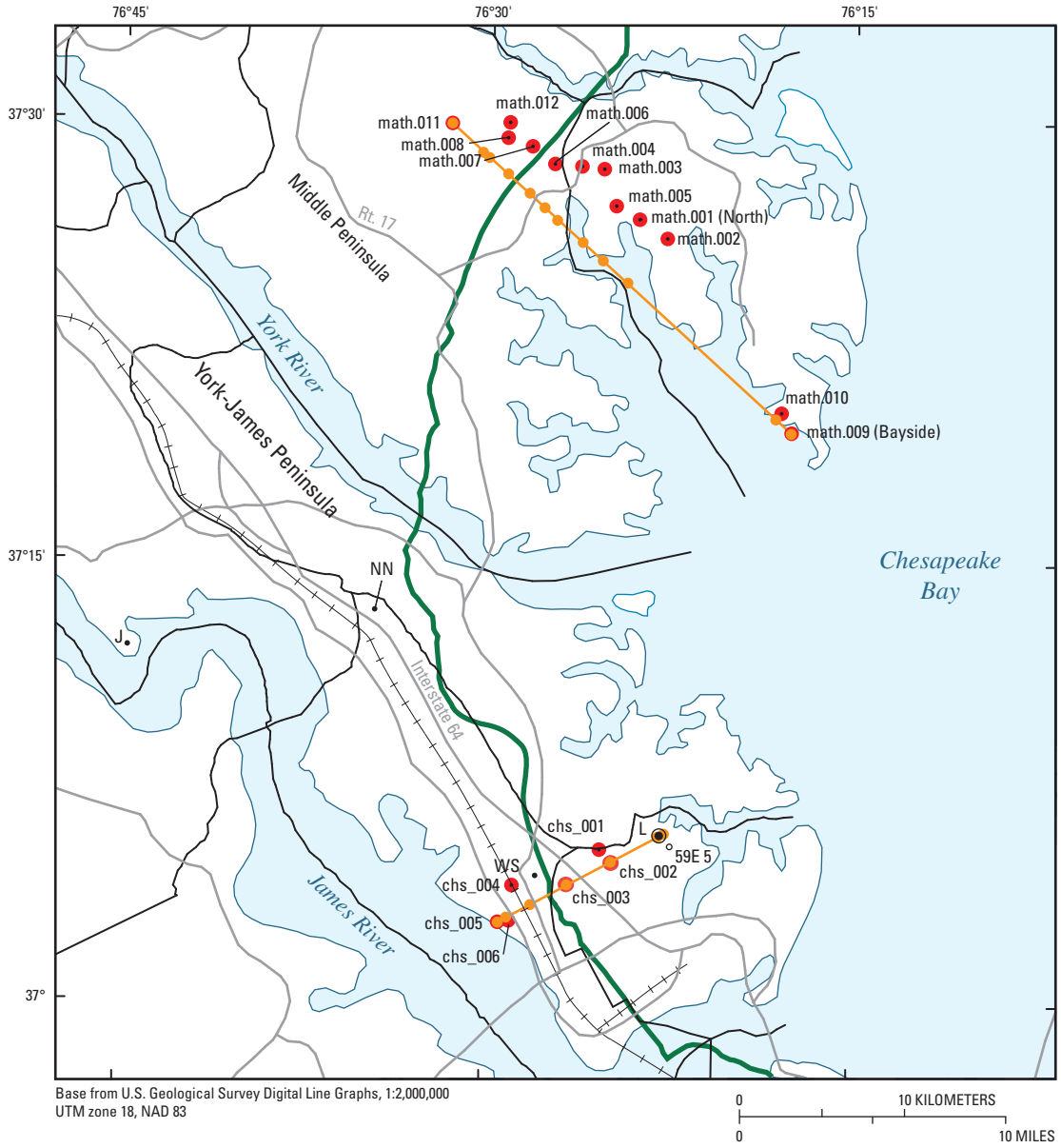

EXPLANATION

Political boundary

Road

Railroad

Outer margin of the Chesapeake Bay impact crater

chs_004 AMT station

Projection of AMT station to section line

COREHOLES AND WELL

J • Jamestown

L ◉ USGS-NASA Langley

NN • Newport News Park 2

WS • Watkins School

59E 5 ○ NASA Langley test well drilled in 1974

Figure J2. Map of the York-James and Middle Peninsulas, Va., showing the locations of 18 AMT stations, part of the outer margin of the Chesapeake Bay impact structure, and coreholes and a well that provided comparison data. Station coordinates and altitudes are given in table J1. Stations having the prefix "chs" were the sites of data collection in 2000 on the York-James Peninsula near the USGS-NASA Langley corehole (L) and the NASA Langley test well drilled in 1974 (59E 5). Stations having the prefix "math" were the sites of data collection in 2001 on the Middle Peninsula near Mathews, Va.; the Bayside corehole coincides with station math.009, and the North corehole coincides with station math.001. Data from the stations were projected onto two electrical section lines; see figs. J7 and J8.

Table J1. Station identifiers, locations, and altitudes for AMT soundings collected in 2000 on the York-James Peninsula (station prefix "chs") and in 2001 on the Middle Peninsula (station prefix "math"), Va.

[Station locations are plotted in figure J2, which is a Universal Transverse Mercator (UTM) projection. Latitude and longitude are in decimal degrees north and west, respectively. UTM coordinates are in meters with a central meridian of –75° and base latitude of 0° (zone 18). Altitude is in meters above mean sea level]

Station	Latitude (°N)	Longitude (°W)	UTM (Northing)	UTM (Easting)	Altitude (m)
chs_001	37.08833	76.42000	4105411	373794	6
chs_002	37.08056	76.41167	4104538	374521	5
chs_003	37.06806	76.44194	4103192	371809	8
chs_004	37.06889	76.47528	4103329	368847	9
chs_005	37.04639	76.48833	4100851	367648	9
chs_006	37.04667	76.48111	4100872	368290	10
math.001	37.44550	76.39810	4145008	376326	8
math.002	37.43471	76.37904	4143786	377994	5
math.003	37.47383	76.42304	4148185	374167	6
math.004	37.47524	76.43845	4148362	372807	5
math.005	37.45307	76.41448	4145869	374889	11
math.006	37.47662	76.45684	4148539	371183	32
math.007	37.48608	76.47239	4149611	369824	24
math.008	37.49088	76.48927	4150166	368340	31
math.009	37.32557	76.29249	4131569	385486	1
math.010	37.33648	76.29958	4132788	384874	2
math.011	37.49886	76.52779	4151107	364949	23
math.012	37.49949	76.48795	4151120	368472	21

Once the phases and resistivities are estimated from the impedances, a Bostick depth transform (Bostick, 1977) is used to transform frequency domain apparent resistivity data into a resistivity-versus-depth sounding. The Bostick depth transforms are calculated for each frequency by using:

$$\rho_{Bostick} = \rho \times \frac{(1+M)}{(1-M)}, \text{where } M = \frac{d\log(\rho)}{d\log(\phi)} \qquad (8)$$

M equals the slope of the apparent resistivity curve on a log-log plot. The slope is estimated by using a finite difference approximation. Another way M can be calculated is to use the Hilbert transform relationship (Sheriff and Geldart, 1982; Sutarno and Vozoff, 1991) between the apparent resistivity ρ and its phase ϕ in degrees translated into the first quadrant and clipped to the range $0° \le \phi \le 90°$:

$$M = 1 - \left(\frac{\phi}{45}\right) \qquad (9)$$

and

$$D_{meters} = \sqrt{\frac{\rho}{2\pi f \mu_0}} \qquad (10)$$

where D_{meters} is depth in meters, and μ_0 is magnetic permeability of free space.

The cross sections can be generated by using the rotationally invariant arithmetic average derived from the full tensor impedances. Arithmetic electrical sections can be computed by using the following formula:

$$Z_{arithmetic} = \frac{(Zxy + Zyx)}{2} \qquad (11)$$

If the geologic structure is two dimensional, then the tensor Z can be rotated to the angle corresponding to the strike of the geology to get a rotated tensor Z'. For Z', $Z'xy$ and $Z'yx$ are maximized and $Z'xx$ and $Z'yy$ are minimized. The angle θ_0 that maximizes:

$$Z'xy^2 + Z'yx^2 \qquad (12)$$

is the principal direction of Z. The principal direction of Z, or the *Zstrike,* is evaluated for each frequency. The way the *Zstrike* is calculated results in four possible solutions at 90° intervals, or two possible geologic strike directions. Because we did not use a vertical magnetic coil, tipper information was unavailable; thus, the choice between these solutions was based on geologic information. A series of impedance polar diagrams with the *Zstrike* calculated for each frequency indicates how the geologic strike varies with frequency.

Results

AMT soundings were made to determine variations in the electrical resistivity of the earth with depth (Spies and Frischknecht, 1991) along two electrical section lines. Both AMT sounding lines cross the curvilinear Suffolk-Big Bethel scarp (Johnson and others, 2001) on the York-James and Middle Peninsulas of the Chesapeake Bay as seen in the digital terrain (shaded-relief) map (fig. J1). The locations where the AMT soundings were collected and lines of electrical sections generated from them are plotted in figure J2. These lines constructed from the AMT stations were designed to cross normal to the outer margin of the annular trough adjacent to the high-resolution seismic profile (Catchings and others, this volume, chap. I) and close to several wells used for ground truth.

Raw AMT resistivity and phase curves were edited, interpolated, and inverted by using the Bostick depth transform. The inverted soundings map the location of the outer margin as a resistivity high. The transition between low-resistivity Lower Cretaceous sediments and the resistive though weathered Paleozoic and Proterozoic crystalline basement is a resistivity gradient. In general, apparent resistivity patterns seen in the sections agree with the geology, induction well logs, and seismic-reflection data. The electrical sections provide an image showing the location of the outer margin of the impact structure and basement contact.

The series of soundings carried out during 2000 and 2001 show similar results, although details of the electrical sections generated from the individual soundings differ in several ways. The soundings collected during the spring of 2000 on the York-James Peninsula were recorded by using an EMI 10-channel receiver. In practice, the receiver requires a total of seven channels per tensor AMT sounding. Channels one through four were *Ex, Ey, Hx,* and *Hy*. The fifth channel, *Hz,* was collected as a null because vertical magnetic sensor data were not collected. Channels six and seven record the remote data channels *Rx* and *Ry*. In this case, data from *Hx* and *Hy* were written to channels six and seven to provide a local reference (*Rx* and *Ry*).

The soundings collected during the spring of 2001 on the Middle Peninsula of the Chesapeake were recorded by using a four-channel Geometrics EH4 receiver. The four channels were *Ex, Ey, Hx,* and *Hy*. The local magnetic reference (*Rx* and *Ry*) was computed by using *Hx* and *Hy* channels.

All the soundings were collected in areas where cultural interference is a problem. Powerlines, roads, sewerlines, and other cultural artifacts make recording difficult, and the setup is subject to assessment of the effects caused by local interfering signals. Electromagnetic signals recorded in urban or suburban settings are typically noisy, and caution must be used to interpret the electrical sections.

To limit the noise generated by cultural effects, both receivers used a 60-Hz notch filter to remove effects caused by the local power grid. For the EMI MT1 system used during 2000, coherency filtering removed signals that had a coefficient of coherence less than 0.8. The Geometrics EH4 system, used during 2001, had a two-stage filter. The EH4 used cutoffs for the coefficient of coherence at 0.3 for the first stage and 0.5 for the second stage. Signal amplitudes were monitored, and any that saturated the receiver amplifiers were rejected. Time series that had more than seven saturations were also rejected. Assessments were made of the sounding locations before and after data collection. Sites were chosen so that stations were 100 m (330 ft) away from known powerlines. The first AMT station collected on the York-James Peninsula, chs_001, was rejected because one electrical field line straddled a buried power conduit that interfered with and degraded the natural-source curves.

Discussion

Both AMT profiles show a zone of higher resistivities coincident with the outer margin. Unedited AMT resistivity plots for each station on the York-James Peninsula transect are shown in figure J3. Unedited AMT resistivity plots for each station on the Middle Peninsula are shown on figure J4. Unedited AMT phase plots for each station on the York-James Peninsula transect are shown in figure J5. Unedited AMT phase plots for each station on the Middle Peninsula are shown on figure J6. Some of the stations display scattered data points and points with large error bars. These problems are to be expected for any electromagnetic survey conducted in an urban area. Fortunately, many frequencies were collected, and the interpreter could deactivate frequencies with large error bars. The resistivity and phase curves were then edited, smoothed, and interpolated prior to inversion and interpretation.

Figure J7 shows the electrical cross section for the York-James Peninsula. This Bostick inversion uses the single *Ex* field and corresponding *Hy* field. The outer margin of the annular trough here is interpreted to coincide with the resistivity high near AMT station chs_004. Neoproterozoic granite (Horton and others, this volume, chap. B) was drilled beneath the sediments at altitudes of –623.9 m (–2,046.8 ft) in the USGS-NASA Langley corehole and –633.7 m (–2,079 ft) in the NASA Langley test well 59E 5 (fig. J7). Seismic-reflection data also show a strong reflector near these altitudes (Catchings and others, this volume, chap. I, fig. I7). The contact between basement rocks and overlying Cretaceous sediments was placed in figure J7 on the basis of borehole resistivity data and core-sample data, which were extrapolated laterally by using the electrical section.

The high resistivities displayed in figure J7 beneath AMT station chs_005 are anomalous and not understood. This station is close to the James River and is near a country club's main building and restaurant at the southwest end of line. Data for

station chs_005 may be compromised by the land-water boundary or by cultural effects. The resistivity high may represent basement rock that is shallower than that drilled in the USGS-NASA Langley corehole and that is related to Powars' (2000) proposed James River structural zone.

Above the basement and just inside (northeast) of the outer margin, the Cretaceous sediments are thought to be large blocks slumped toward the center of the crater and covered by the Exmore beds (Gohn and others, this volume, chap. C) and postimpact sediments (Powars and others, this volume, chap. G). The resolution in this section is not sufficient to map individual blocks.

Figure J8 shows the resistivity profile on the Middle Peninsula near Mathews, Va. This profile is the directionally invariant arithmetic average calculated (equation 11) from the two measured directions *Ex* and *Ey*. The outer margin of the impact structure along this line coincides approximately with the Suffolk-Big Bethel scarp (Johnson and others, 2001) and stations math.006 and math.007, where a resistivity high extends from basement toward the surface. Resistivities in the sediments are low on both sides of the high interpreted as the outer margin and limit the depth of exploration in some places to 300 m (980 ft). The Bayside corehole (which coincides with station math.009) was drilled during 2001 and penetrated the granitic basement rocks at an altitude of –707.7 m (–2,321.7 ft). The deepest part of the AMT profile reaches the basement in several places, and the basement's top appears to be uneven.

Southeast of stations math.006 and math.007, slumped Cretaceous megablocks are thought to lie above the basement and below the Exmore beds and postimpact sediments. The inverted AMT data do not have the resolution necessary to map individual slumped blocks.

Although the high-resistivity zone that appears near the outer margin on both electrical sections (figs. J7 and J8) is not well understood, it provides enough resistivity contrast to map the outer margin at least on the western and southwestern side of the Chesapeake Bay impact structure. The resistivity high may be caused by freshwater discharging from the Lower Cretaceous sediments at the outer margin, by cementation along the fault zone, or by compaction of the sediments as a result of the impact event. Gubins and Strangway (1978) found similar results while working on the Dumas and Viewfield astroblemes in Saskatchewan: "AMT soundings show in general that these structures are highly resistive in a conductive medium." They also proposed that "to account for the structures being resistive[,] ground water in pore-spaces and fractures must be negligible."

The outer margin of the Chesapeake Bay impact structure is a concentric fault zone that cuts Cretaceous sediments (Poag, 1996). If the westernmost side of the fault zone is normal to the west-to-east regional ground-water flow, then the marginal fault may have provided a permeable zone where water fresher than the brackish water in Chesapeake Bay discharged from the Lower Cretaceous sediments. The resistivity high associated with the marginal fault zone may be caused by the ongoing discharge of freshwater. Alternatively, the resistivity high could be an artifact of the paleo-ground-water flow system; that is, water flowing through the higher permeability material along the ring fracture during the last 35 million years deposited minerals such as SiO_2 and $CaCO_3$ and partially cemented the rocks along and near the fractures. The high could also be caused by some combination of the two processes and impact-related compaction. Further research is needed to resolve this problem.

If the geology is close to a two-dimensional feature such as a vertical fault or vertical contact between different rocks**,** then the impedance tensor *Z* can be rotated to the angle corresponding to the strike of geologic structures (such as fractures) at each frequency to get a rotated tensor *Z´*. Figures J9 and J10 show polar plots of ellipses generated when the *Zxy* tensor impedances are maximized (aqua ellipses) and the corresponding *Zxx* tensor impedances are minimized (pink ellipses). The angle for each frequency that maximizes $(Z'xy^2 + Z'yx^2)$ is called the principal direction of *Z* and is related to the geologic strike. Interpreting the strike directions requires care because the way the strike is calculated results in a 90° ambiguity; the direction it points corresponds to either a minimum or maximum of *Zxy*.

In homogeneous and isotropic (one-dimensional) geologic settings, polar plots of *Zxy* become circular, and the principal strike angle becomes mathematically unresolvable. Where the geology is two dimensional, the *Zxy* plot becomes elliptical, and the *Zxx* plot approaches a minimum. As the sounding depth of investigation or physical location of the sounding approaches a complex three-dimensional geologic structure, the *Zxx* impedance (pink ellipse) cannot be minimized (figs. J9 and J10). Where the geology is moderately complex, the polar plots take on a peanut shape. Where the geology is extremely complex, the polar plots appear first as bowties and then as large cloverleaves. This type of response can also occur where the data are compromised by coherent noise. Cultural noise and land-water boundary conditions near Chesapeake Bay also contribute to the occasional problems in calculating the principal impedance strike direction.

In general, the principal directions of *Z*, or strike of geologic structures, for the York-James Peninsula are to the northwest (fig. J9). The principal directions of *Z* for the Middle Peninsula are to the northeast (fig. J10). These directions are consistent with fractures parallel to a circular impact structure having a northwest strike on the York-James Peninsula and a northeast strike on the Middle Peninsula (fig. J1).

Text continues on p. J16.

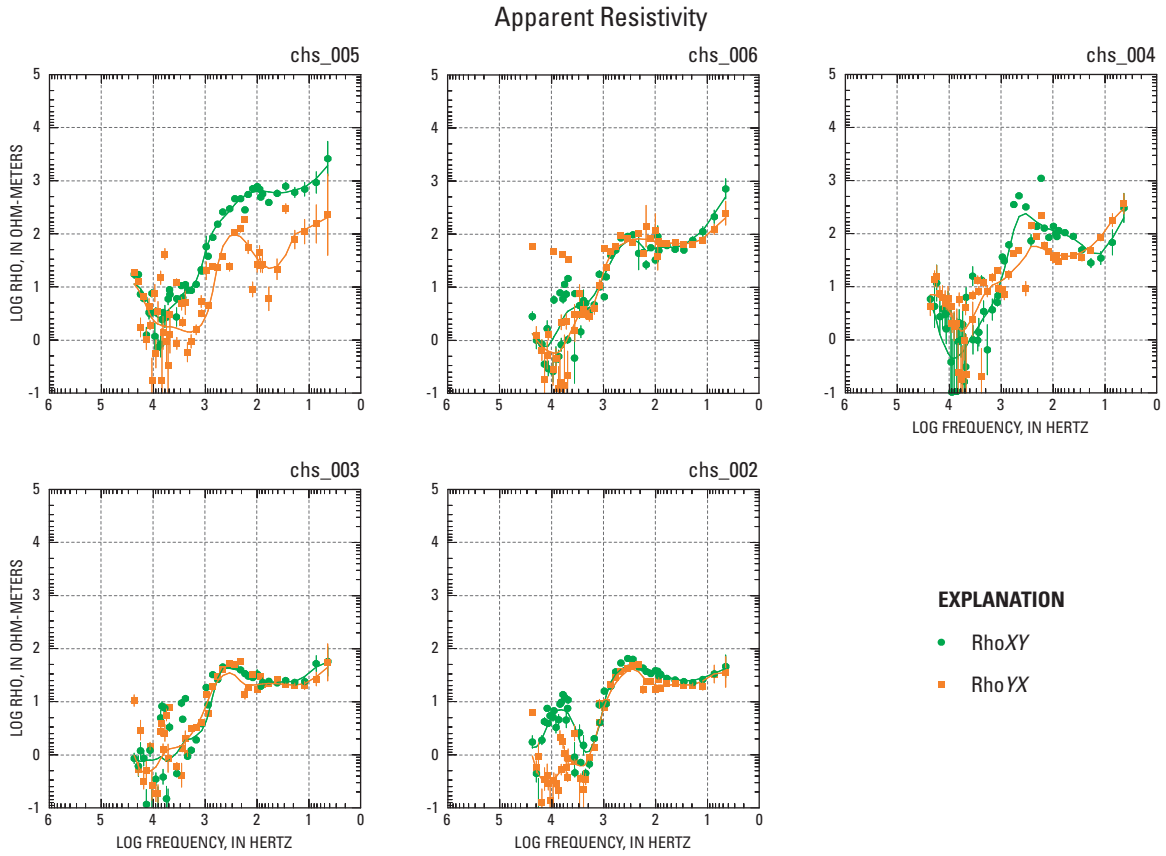

Figure J3. Raw apparent resistivity (ρ, rho) plots of the AMT data collected across the York-James Peninsula, Va., during the spring of 2000. Station locations are shown in figure J2. Data from station chs_001 were rejected because of interference from a buried power conduit. Vertical lines are error bars showing the variance computed by using the method of Gamble and others (1979a). Variables: rho*XY*, resistivity with the electrical (*E*) field in the *x*-direction and the magnetic (*H*) field in the *y*-direction; rho*YX*, resistivity with *E* in the *y*-direction and *H* in the *x*-direction.

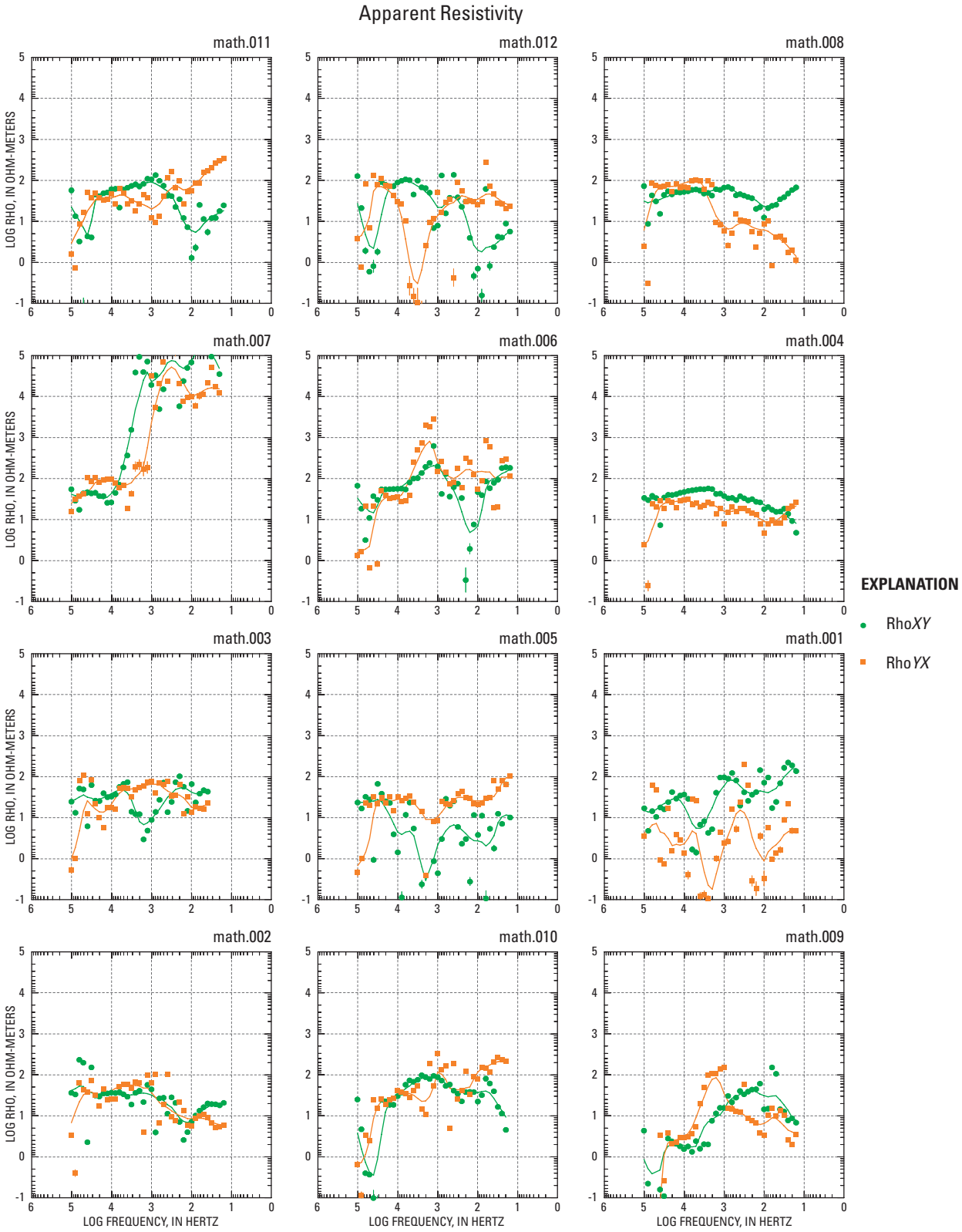

Figure J4. Raw apparent resistivity (ρ, rho) plots of the AMT data collected on the Middle Peninsula near Mathews, Va., during the spring of 2001. Station locations are shown in figure J2, and the sequence of stations along the line of section dictates the order of graphs in this figure. Vertical lines are error bars showing the variance computed by using the method of Gamble and others (1979a). Variables: rho*XY*, resistivity with the electrical (*E*) field in the *x*-direction and the magnetic (*H*) field in the *y*-direction; rho*YX*, resistivity with *E* in the *y*-direction and *H* in the *x*-direction.

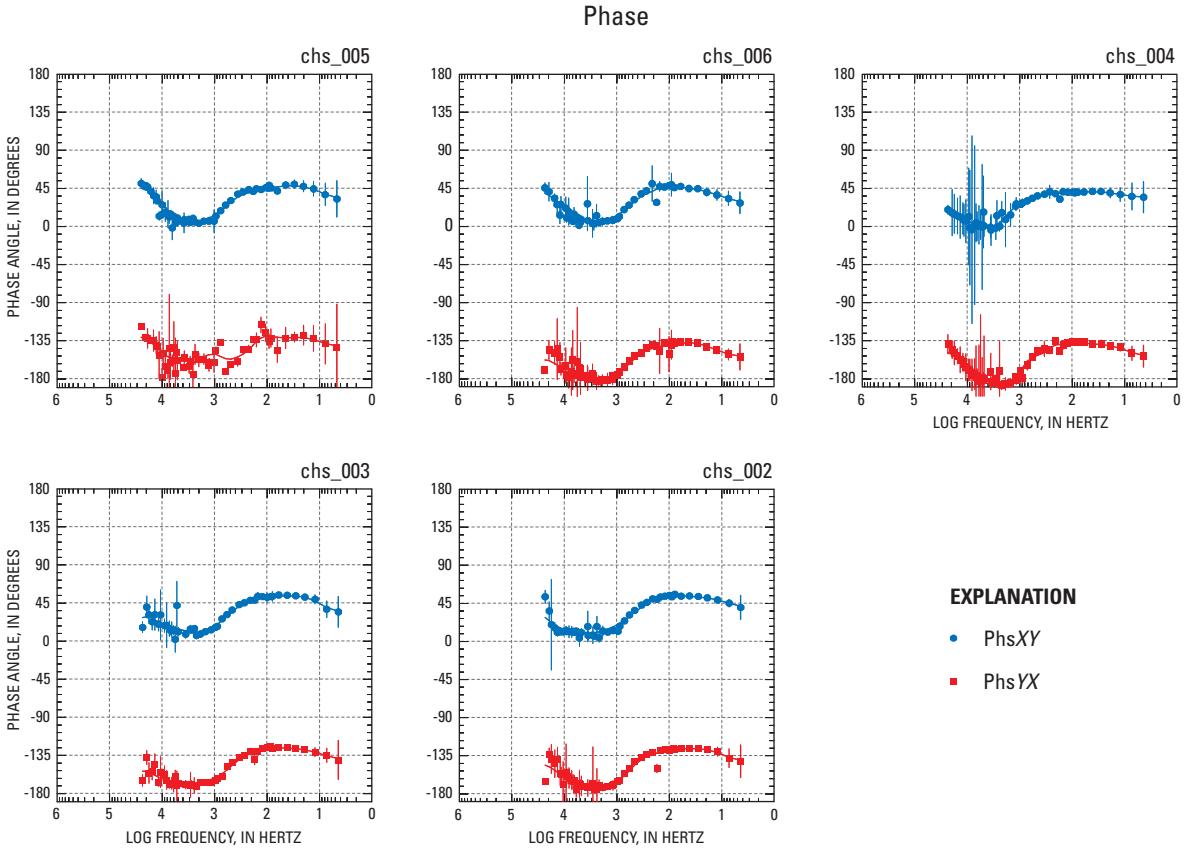

Figure J5. Raw phase (phs) plots of the AMT data collected across the York-James Peninsula, Va., during the spring of 2000. Station locations are shown in figure J2. Data from station chs_001 were rejected because of interference from a buried power conduit. Vertical lines are error bars showing the variance computed by using the method of Gamble and others (1979a). Variables: phs*XY*, phase of the two directions with the electrical (*E*) field in the *x*-direction and the magnetic (*H*) field in the *y*-direction; phs*YX*, phase of the two directions with *E* in the *y*-direction and *H* in the *x*-direction.

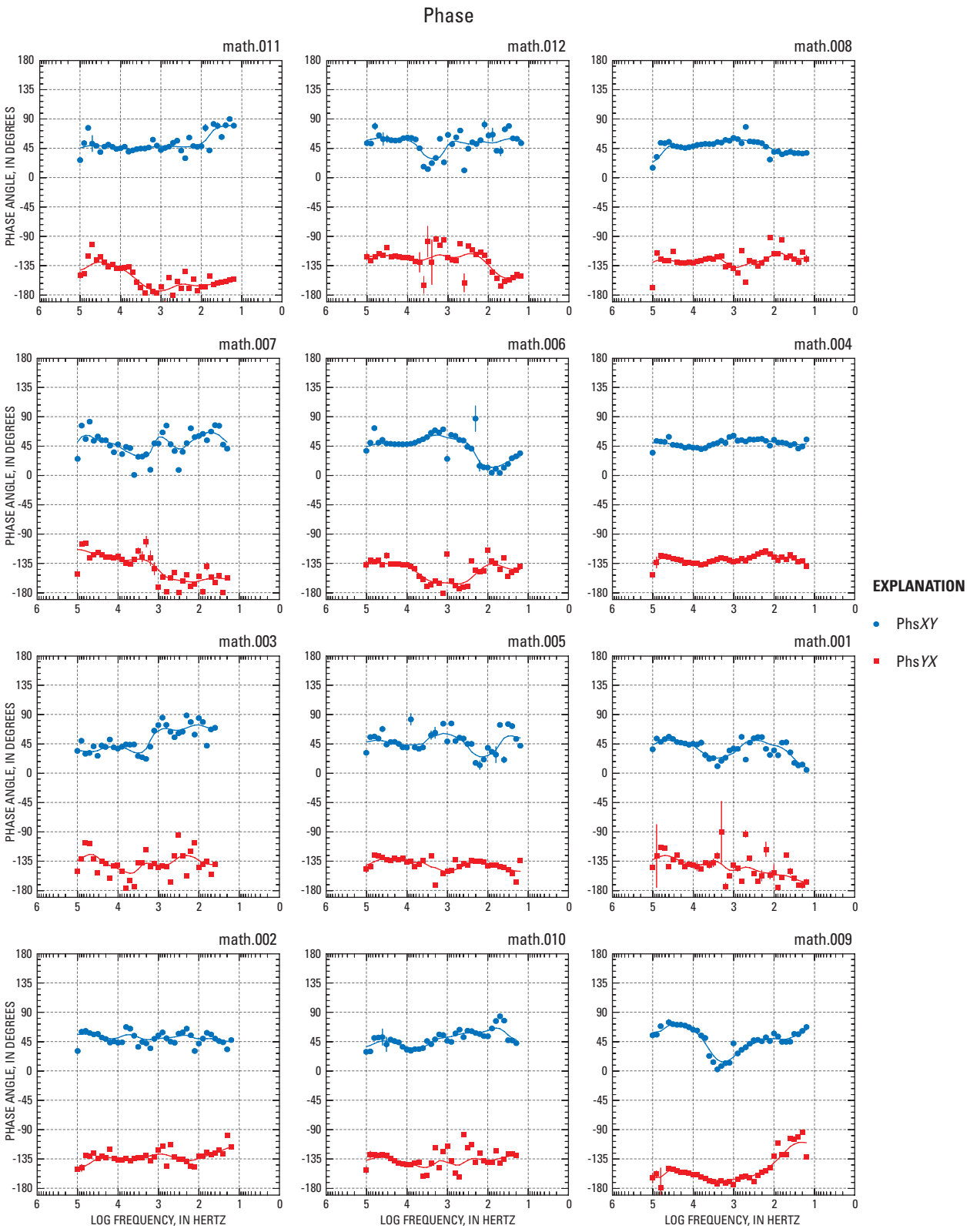

Figure J6. Raw phase (phs) plots of the AMT data collected on the Middle Peninsula near Mathews, Va., during the spring of 2001. Station locations are shown in figure J2, and the sequence of stations along the line of section dictates the order of graphs in this figure. Vertical lines are error bars showing the variance computed by using the method of Gamble and others (1979a). Variables: phs*XY*, phase of the two directions with the electrical (*E*) field in the *x*-direction and the magnetic (*H*) field in the *y*-direction; phs*YX*, phase of the two directions with *E* in the *y*-direction and *H* in the *x*-direction.

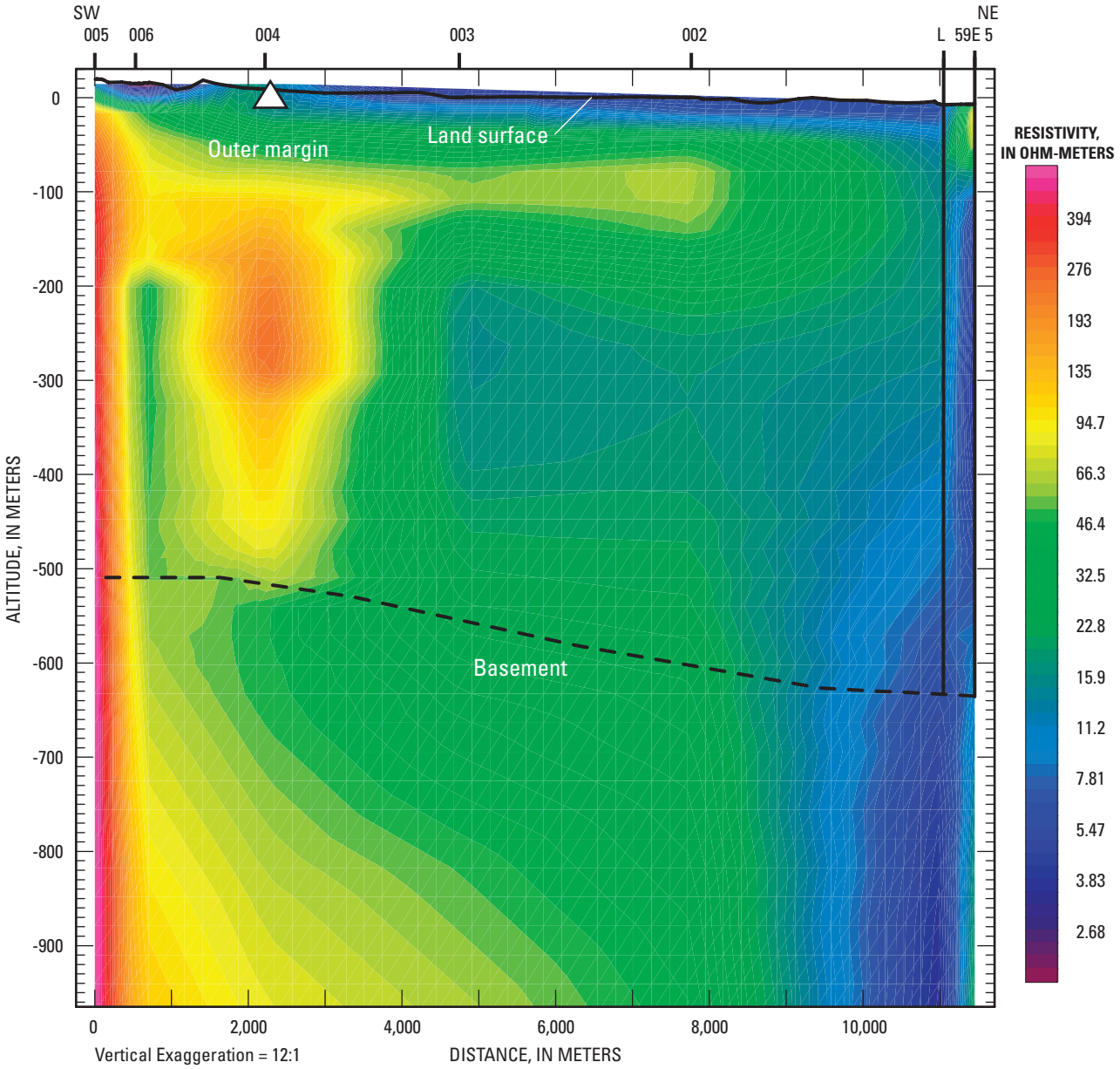

Figure J7. Bostick inverted electrical resistivity section with the electrical (*E*) field in the *x*-direction and the magnetic (*H*) field in the *y*-direction across the York-James Peninsula, Va. The strike of the section is N. 61° E. AMT station locations are shown in figure J2; to save space, the station numbers 002–006 across the top of the section lack the prefix "chs_." The two stations at the right side of the section are at the National Aeronautics and Space Administration (NASA) Langley Research Center in Hampton, Va.: the USGS-NASA Langley corehole (L), which was drilled in 2000, and the NASA Langley test well (59E 5), which was drilled in 1974; see Powars and others (this volume, chap. G, fig. G4). The resistivity data from the two holes at Langley were generated from induction borehole log data (the 2000 log is given by Powars and others, this volume, chap. G, fig. G7; the 1974 log is unpub. data on file at the Richmond, Va., office of the USGS). The altitude is shown in meters below mean sea level. The contact at the top of basement rocks is based upon the granite contacts drilled in the 1974 and 2000 wells extrapolated to the southwest. The depth of granite in the 1974 well was given by Johnson (1975, table 1) as 636 m (2,088 ft), which was corrected to an altitude of –633.7 m (–2,079 ft) (D.S. Powars, USGS, written commun., 2005); the depth of granite in the 2000 well (Horton and others, this volume, chap. B) was converted to an altitude of –623.9 m (–2,046.8 ft). The interpreted location of the outer margin of the Chesapeake Bay impact structure coincides with the resistivity high near station chs_004.

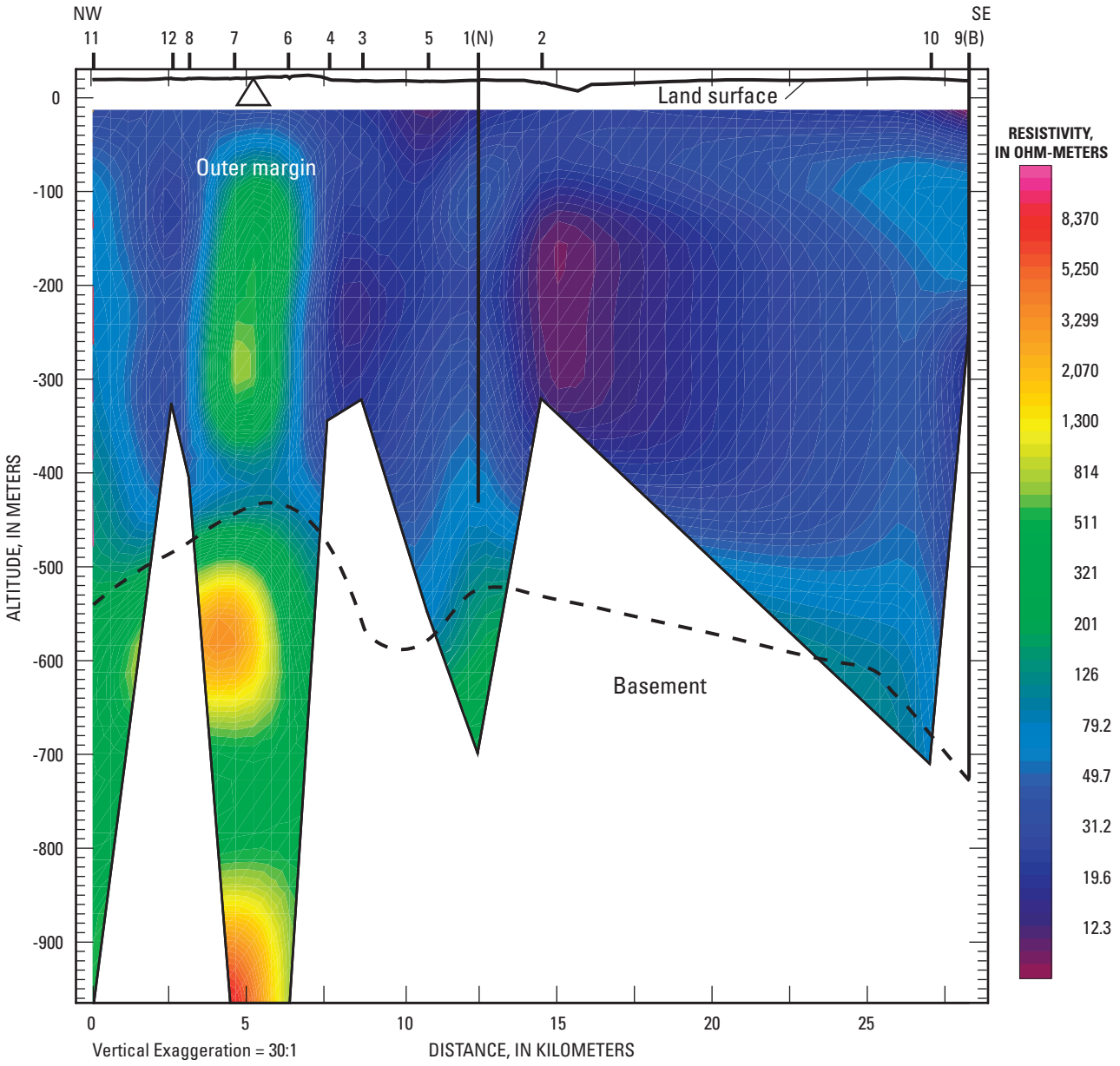

Figure J8. Bostick depth section showing a plot of arithmetic average resistivities computed from the two directions (*Ex* and *Ey*) across the Middle Peninsula, Va. The strike of the section is S. 46° E. AMT station locations are shown in figure J2; to save space, the station numbers across the top of the section lack the prefix "math.0." The altitude is shown in meters below mean sea level. Depth of the colored resistivity cross section is limited by low resistivities encountered in the near surface. The North (N) corehole coincides with AMT station math.001, and the Bayside (B) corehole coincides with AMT station math.009; both coreholes were drilled by the USGS in 2001. The Bayside corehole penetrated the Cretaceous sediment contact with the granite basement at an altitude of –707.7 m (–2,321.7 ft). The bottom of the North corehole at an altitude of –430.5 m (–1,412.5 ft) did not penetrate the granite basement. The dashed line is the basement contact interpreted by using the Bayside and North coreholes as ground truth. The interpreted location of the outer margin of the Chesapeake Bay impact structure coincides with the resistivity high measured at AMT stations math.006 and math.007 and with the Suffolk-Big Bethel scarp identified in figure J1.

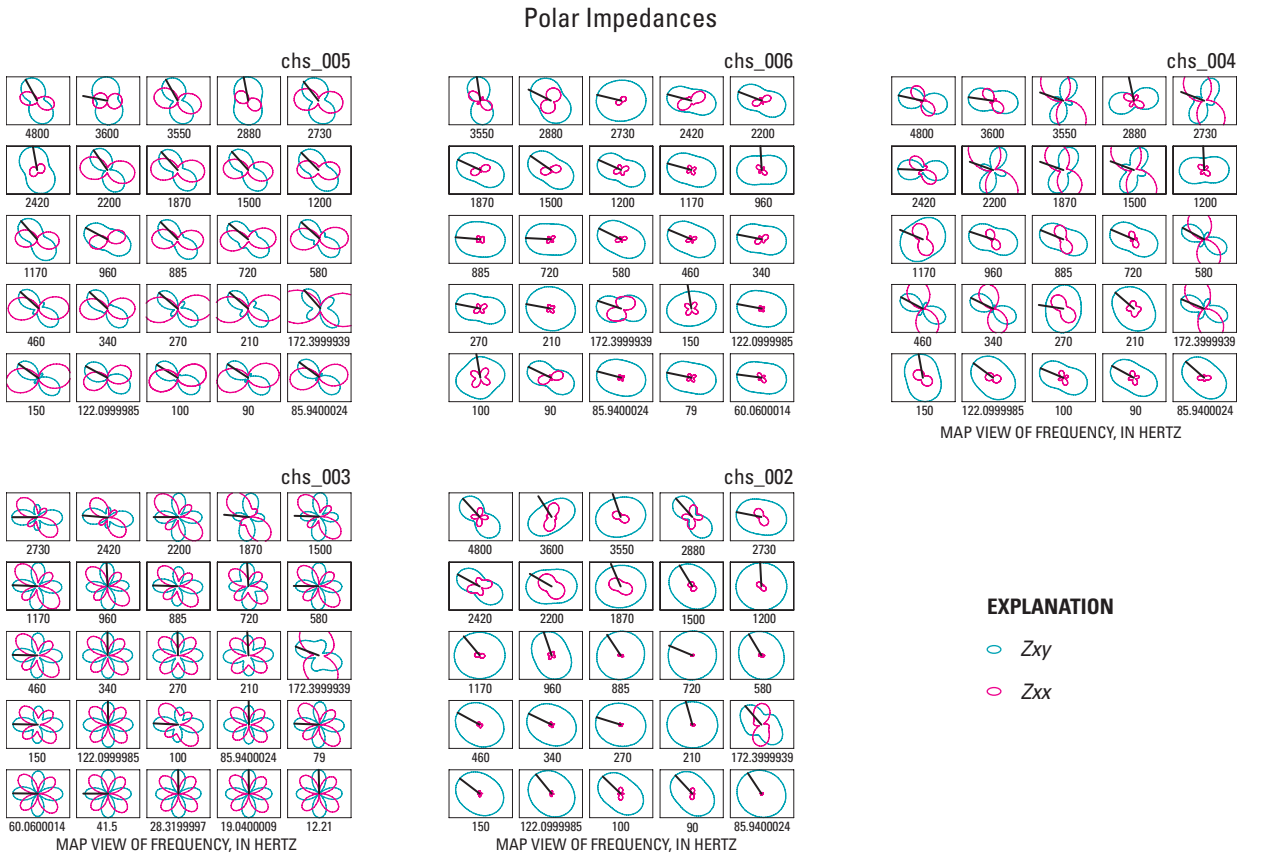

Figure J9. Polar impedance and impedance strike plots for the stations (fig. J2) where AMT data were collected across the York-James Peninsula, Va., during the spring of 2000. For each station, data are plotted for 25 different frequencies selected to show the largest spread. *Zxy* tensor impedances (aqua ellipses) are maximized, and corresponding *Zxx* tensor impedances (pink ellipses) are minimized. The black line that originates at the center of each polar-plot ellipse represents the principal impedance strike direction. North is at the top of the page.

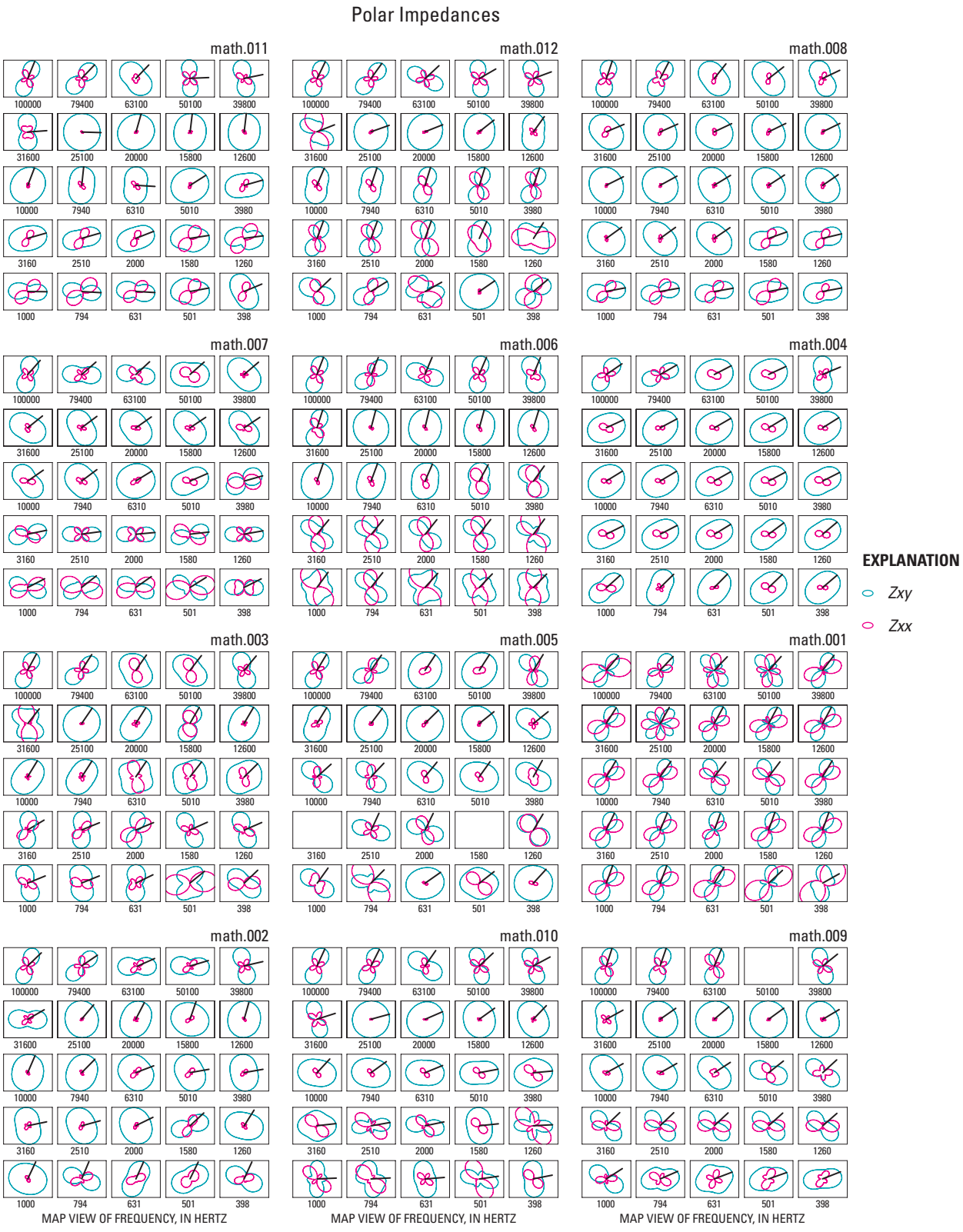

Figure J10. Polar impedance and impedance strike plots for the stations (fig. J2) where AMT data were collected on the Middle Peninsula near Mathews, Va., during the spring of 2001. For each station, data are plotted for 25 different frequencies to show the largest spread. Blank plots indicate inactive frequencies. *Zxy* tensor impedances (aqua ellipses) are maximized, and corresponding *Zxx* tensor impedances (pink ellipses) are minimized. The black line that originates at the center of each polar-plot ellipse represents the principal impedance strike direction. North is at the top of the page.

Conclusions

A resistivity contrast in sediments near the outer margin of the Chesapeake Bay impact structure measured on both the York-James Peninsula and the Middle Peninsula AMT profiles can be used to map the location of the outer margin of the impact structure. The reason the resistivity contrast exists and is associated with the outer margin is not clearly understood but may be attributed to a combination of freshwater intrusion, cementation, or impact-related compaction. Although electromagnetic readings in urban and suburban areas are typically noisy, useful resistivity profiles can be obtained in these areas if care is taken in selecting station locations.

In places, the depth of exploration was great enough to map the lateral contact between Cretaceous sediments and Proterozoic and Paleozoic basement rocks. The basement contact, however, was close to the limit of the technique's resolution and depth of exploration, especially near Mathews, Va.; in that area, low resistivities in the near-surface sediments limited the depth of exploration. Three-dimensional structures in Cretaceous sediments above the basement contact and within the annular trough probably lack contrasts in resistivity and thus could not be imaged well enough to suggest shapes such as slumped megablocks.

Polar plots generated for AMT stations on the York-James Peninsula indicate that the strike is to the northwest. Polar plots for AMT stations on the Middle Peninsula indicate a strike to the northeast. The principal directions for the impedance strike trends are generally consistent with fractures parallel to the curvilinear trend of the outer margin, with exceptions for stations near the brackish water in Chesapeake Bay.

Acknowledgments

U.S. Geological Survey (USGS) investigations of the Chesapeake Bay impact structure are conducted in cooperation with the Hampton Roads Planning District Commission, the Virginia Department of Environmental Quality, and the National Aeronautics and Space Administration (NASA) Langley Research Center. I extend a special thanks to Matt Smith (USGS), Professor Gerald H. Johnson (of the Department of Geology of the College of William and Mary), Professor Rick Berquist (of the Department of Geology of the College of William and Mary), and his students, Tim Russel and Heidi Romine, without whose field help this work would have been much harder.

References Cited

Bostick, F.X., Jr., 1977, A simple and almost exact method of MT analysis, *in* Workshop on Electrical Methods in Geothermal Exploration: Salt Lake City, Utah, University of Utah, p. 175–177. (Prepared under USGS contract 14–08–0001–G–359.)

Cagniard, Louis, 1950, Procédé de prospection géophysique [Procedure of geophysical prospecting]: French patent no. 1025683, 6 p., available online at http://l2.espacenet.com/espacenet/bnsviewer?CY=ep&LG=en&DB=EPD&PN=FR1025683&ID=FR+++1025683A++I+

Cagniard, Louis, 1953, Basic theory of the magneto-telluric method of geophysical prospecting: Geophysics, v. 18, no. 3, p. 605–635.

Dmitriev, V.I., and Berdichevsky, M.N., 1979, The fundamental model of magnetotelluric sounding: Proceedings of the IEEE (Institute of Electrical and Electronics Engineers), v. 67, no. 7, p. 1034–1044.

Gamble, T.D., Goubau, W.M., and Clarke, J., 1979a, Error analysis for remote reference magnetotellurics: Geophysics, v. 44, no. 5, p. 959–968.

Gamble, T.D., Goubau, W.M., and Clarke, J., 1979b, Magnetotellurics with a remote magnetic reference: Geophysics, v. 44, no. 1, p. 53–68.

Gubins, A., and Strangway, D.W., 1978, Magnetic and audio frequency magnetotelluric (AMT) investigations at the Dumas and Viewfield, Saskatchewan astroblemes [abs.]: Eos, Transactions, American Geophysical Union, v. 59, no. 12, p. 1036.

Hoover, D.B., Frischknecht, F.C., and Tippens, C.L., 1976, Audiomagnetotelluric sounding as a reconnaissance exploration technique in Long Valley, California: Journal of Geophysical Research, v. 81, no. 5, p. 801–809.

Hoover, D.B., and Long, C.L., 1976, Audio-magnetotelluric methods in reconnaissance geothermal exploration: United Nations Symposium on the Development and Use of Geothermal Resources, 2d, San Francisco, Calif., 20–29 May 1975, Proceedings, v. 2, p. 1059–1064.

Hoover, D.B., Long, C.L., and Senterfit, R.M., 1978, Some results from audiomagnetotelluric investigations in geothermal areas: Geophysics, v. 43, no. 7, p. 1501–1514.

Johnson, G.H., Powars, D.S., Bruce, T.S., Beach, T.A., Harris, M.S., and Goodwin, B.K., 2001, Post-impact effects of the Eocene Chesapeake Bay impact, lower York-James Peninsula, Virginia: Virginia Geological Field Conference, 31st, Williamsburg, Virginia, October 19 and 20, 2001 [Guidebook], 40 p.

Johnson, S.S., 1975, Bouger gravity in southeastern Virginia: Virginia Division of Mineral Resources Report of Investigations 39, 42 p.

Keller, G.V., and Frischknecht, F.C., 1966, Electrical methods in geophysical prospecting: London, Pergamon Press, 519 p.

Poag, C.W., 1996, Structural outer rim of Chesapeake Bay impact crater—Seismic and bore hole evidence: Meteoritics & Planetary Science, v. 31, no. 2, p. 218–226.

Poag, C.W., Hutchinson, D.R., Colman, S.M., and Lee, M.W., 1999, Seismic expression of the Chesapeake Bay impact crater; Structural and morphologic refinements based on new seismic data, *in* Dressler, B.O., and Sharpton, V.L., eds., Large meteorite impacts and planetary evolution; II: Geological Society of America Special Paper 339, p. 149–164.

Poag, C.W., Plescia, J.B., and Molzer, P.C., 1999, Chesapeake Bay impact structure; Geology and geophysics [abs.], *in* Gersonde, Rainer, and Deutsch, Alexander, eds., Oceanic impacts; Mechanisms and environmental perturbations; ESF–IMPACT Workshop, April 15–April 17, 1999, Alfred Wegener Institute for Polar and Marine Research, Bremerhaven, Germany, Abstracts: Berichte zur Polarforschung (Reports on Polar Research), v. 343, p. 79–83.

Powars, D.S., 2000, The effects of the Chesapeake Bay impact crater on the geologic framework and the correlation of the hydrogeologic units of southeastern Virginia, south of the James River: U.S. Geological Survey Professional Paper 1622, 53 p., 1 oversize pl. (Also available online at http://pubs.usgs.gov/prof/p1622)

Powars, D.S., and Bruce, T.S., 1999, The effects of the Chesapeake Bay impact crater on the geological framework and correlation of hydrogeologic units of the lower York-James Peninsula, Virginia: U.S. Geological Survey Professional Paper 1612, 82 p., 9 oversize pls. (Also available online at http://pubs.usgs.gov/prof/1612)

Sheriff, R.E., and Geldart, L.P., 1982, History, theory, and data acquisition, v. 1 *of* Exploration seismology: Cambridge, U.K., Cambridge University Press, 253 p.

Spies, B.R., and Frischknecht, F.C., 1991, Electromagnetic sounding, *in* Nabighian, M.N., and Corbett, J.D., eds., Electromagnetic methods in applied geophysics: Society of Exploration Geophysicists Investigations in Geophysics no. 3, v. 2 (Applications), pt. A, p. 285–422.

Sutarno, Doddy, and Vozoff, Keeva, 1991, An application of regression *M*-estimation with the Hilbert transform to magnetotelluric data processing: Exploration Geophysics, v. 22, no. 2, p. 383–389.

Vozoff, Keeva, 1986, Magnetotelluric methods: Society of Exploration Geophysicists Geophysics Reprint Series no. 5, 763 p.

Vozoff, Keeva, 1991, The magnetotelluric method, *in* Nabighian, M.N., and Corbett, J.D., eds., Electromagnetic methods in applied geophysics: Society of Exploration Geophysicists Investigations in Geophysics no. 3, v. 2 (Applications), pt. A, p. 641–712.

Wait, J.R., 1962, Theory of magnetotelluric fields: U.S. National Bureau of Standards Journal of Research, Radio Propagation, v. 66D, p. 509–541.